Phase Recovery for 3D SAR Range Focusing

Mehrdad Yaghoobi, *Member, IEEE,* and Shaun I. Kelly, *Member, IEEE,* and Mike E. Davies, *Fellow, IEEE*

Summary

The problem of calibrating Synthetic Aperture Radar (SAR) data for 3D image formation will be investigated here. A source of errors in modern radar systems is inaccurate range estimations, during the data collection. This is caused by two ambiguities in the platform location and the scene topography map. Such range estimation errors induce some asynchronization in the dechirping process, *i.e.* a shift in the range direction. When such an error is small, the final image will be blurred and possibly compensated using conventional autofocus techniques. In multipass SAR image formation, this error between the passes is large and we need a different machinery to correct it.

We formulate the problem of SAR pulse compression with the range estimation error, in a general setting. The range estimation error appears as some structured phase error in the phase history. We then introduce a new phase recovery technique for compensating the phase error. Some simulation results show the capabilities of the introduced method.

Extended Abstract

The main principle of SAR systems is to generate a synthetic aperture, using a moving platform and collect the pulse information from different spacial locations. The accurate knowledge of location of the platform and the scene topography is the necessary part of a high resolution SAR image formation. However, none of these two information are precisely known for various reasons, including an inaccuracy of the navigation systems and the imaging of an unknown area. The conventional approach to calibrate the location information is to use some reference targets *with the ground truth information about their locations*. While such techniques are generally successful, such reference targets may not exist in the real experiments or the precise location is unknown. As a result, many digital focusing techniques, *i.e.* called the autofocus techniques, have been proposed, including Phase Gradient Algorithm (PGA) [1], map drift [2], [3] and sparsity based autofocus [4], [5] techniques. In these techniques, we often assume a small aperture, a far-field setting and/or small errors [6]. As a result, such techniques have limitations in the wide-angle, with a large error and possibly digitally chipped SAR image [7]. Particularly, any autofocus techniques, based on the single phase error per pulse model, *i.e.* the most frequent approach for single pass SAR autofocus, cannot correctly compensate the range error, when it is larger than $\lambda/16$, where λ is the wavelenght [6], [8].

3D-SAR imaging needs a new set of autofocus techniques which incorporates the multipass nature of the trials [9], to compensate relatively larger range errors [7]. The most intuitive approach is to extend the prominent point autofocus techniques to a three-dimensional setting [10]. This approach needs to have a single dominant bright target in the scene to aligned the pulses with respect to the range compressed peaks. An extension of such a technique is to use multiple Quad-Trihedral (QT) corner reflectors to correct the location of the platform [11]. Another approach is to use a parametric frequency domain linear filter and adaptively find the parameters [8], [12].

In this work, we reformulate the effect of the range estimation error, and show that such an error appears as a structured phase error in the phase history. We then tackle this problem by formulating it as a phase retrieval problem. Inspired by the Gerchberg-Saxton phase recovery algorithm, we introduce an easy range estimation error correction technique for multipass SAR imaging. We also discuss about the necessary and preferred settings which allow us to successfully recover the range estimation errors, in terms of phase errors. Some simulation results will be presented to demonstrate the success of the algorithm in a (controlled) synthetic and a real data experiment.

A. Formulation

Let the reflectivity map of the scene be $\mathbf{X}$ and the linear (forward) operator, which maps the scene reflectivity to the phase history, be noted by $\mathcal{A} : \mathcal{C}^{N\times N} \rightarrow \mathcal{C}^{M\times J}$, where M is the range compressed pulse length and J is the number of pulses. This operator includes the range compression of the pulses generating phase history $\mathbf{R}$, with range compressed pulses as its columns. The range estimation error appears as a delay/forward-shift before dechirping process. As a result, we encounter some structured phase shifts in each compressed pulse, *i.e.* $\epsilon_j = \frac{2}{c}\delta R_j$ where c is the speed of light in the free space and δR_j is the range estimation error. A mathematical formulation of this phenomenon can be presented by an element by element phase shift, *i.e.* $\mathbf{R}_{\boldsymbol{\epsilon}} = \boldsymbol{\Gamma} \odot \mathcal{A}\mathbf{X}$, where $\odot$ is the element-by-element multiplication, $\boldsymbol{\epsilon} = [\epsilon_j]$ and $\boldsymbol{\Gamma} = [\boldsymbol{\gamma}_j]_{j\in\mathcal{J}}$ is defined as follows,

$$\{\boldsymbol{\gamma}_j\}_m = \exp\left(-i(\zeta(\epsilon_j)\, m + \eta(\epsilon_j))\right), \tag{1}$$

where $\zeta(\epsilon_j) = \alpha\epsilon_j\Delta t$ and $\eta(\epsilon_j) = \epsilon_j(\omega_0 - \alpha\tau_0 - \frac{\alpha\epsilon_j}{2})$ are some functions of ϵ_j and independent of m, where α is the chirp rate, Δt is the sampling interval, ω_0 is the starting frequency of the pulses and τ_0 is the round trip delay to the scene centre. The conventional autofocus methods ignore the term based on m and only consider a single phase error for each pulse, *i.e.* $\eta(\epsilon_j)$. Such methods work well when the range estimation errors are small compared to the range cell size. In other words, they are not designed to correct the reflectivity map, when it needs to move a peak from one range cell to another [1].

Compensation of a large range error, which can be observed in various publicly available 3D-SAR databases [7], [10], needs a new machinery to cope with such a phase error correction. Some of canonical autofocus techniques, which have been used for range estimation error compensation, are based on gradually focusing the image using a gradient descent technique, *e.g.* PGA and sparsity based autofocus. We here present a fundamentally different approach which can solve the problems with much larger range estimation errors. The new approach is based on the reformulation of the problem and solving with a canonical technique called Grechberg-Saxton (GS) or error reduction algorithm [13].

GS algorithm is based on the assumption that phase of an observation system in Fourier domain has been disrupted. On the other hand,

MY and MED are with the Institute for Digital Communication and with the Joint Research Institute for Signal and Image Processing, Edinburgh University, Kings Buildings, Mayfield Road, Edinburgh EH9 3JL, UK (e-mail: yaghoobi@ieee.org, mike.davies@ed.ac.uk). SIK is with Blackmagic Design, Australia. shaun.i.kelly@gmail.com

This work was supported by EPSRC grants EP/K014277/1 and the MOD University Defence Research Collaboration in Signal Processing.

978-1-5090-0863-6/16/$31.00 ©2016 IEEE

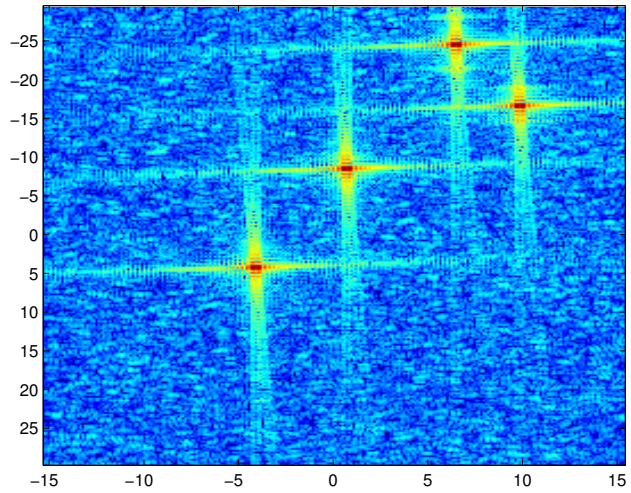

Fig. 1. Backprojection of unfocussed phase history.

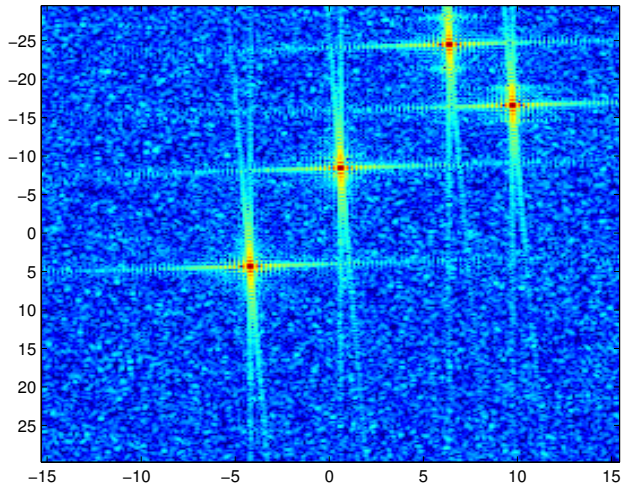

Fig. 3. SAR image after range focusing.

we have some prior information about what has been measured in time and frequency domains. We can then use an iterative method alternating between time and frequency domains and enforcing the prior information as some constrains. A schematic diagram of GS algorithm has been shown in Figure 2. Some conventional constraints for the signals in the time/space domain are to be real, bounded and/or structured and the Frequency domain to be band-limited and have particular magnitudes.

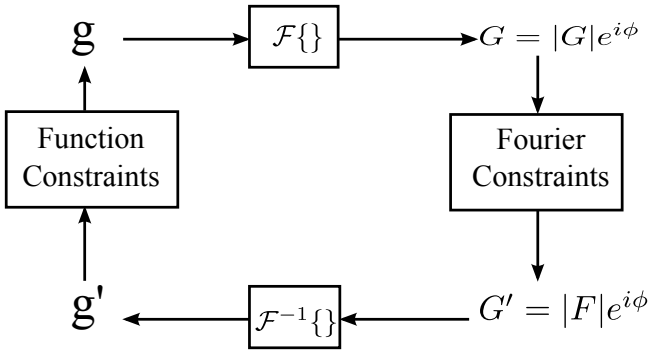

Fig. 2. Gerchberg-Saxton (error reduction) algorithm.

The SAR forward operator is not Fourier or a unitary operator. As a result, such an iterative scheme cannot be used in its original form. We introduce a modified algorithm, inspired from GS method, in the next subsection.

B. Range Estimation Error Reduction with a Phase Recovery Technique

When the measurements of a system are linear with some phase ambiguity, which includes the case of completely losing the phase information, we need some phase recovery techniques. Such techniques use the fact that the system has some properties, including linearity, harmonicity, randomness or an overdetermined nature, and the signal of interest has some properties in spatial/time and/or frequency domain. Such features of the sensing system and the signals have helped researchers of various fields to introduce fundamentally different phase recovery algorithms [13]. While some attention have recently been given to the convex and gradient based techniques, they are not often practical for real size problems [14]. We here introduce a practical iterative phase recovery algorithm for the recovery of $\mathbf{\Gamma}$, which is structurally similar to the standard form of GS algorithm. The schematic of the GS algorithm is presented in Figure 2. We normally start from one point of the loop, which is more convenient for our sensing structure, and continue until convergence. GS iteratively calculates the Fourier, respectively inverse Fourier, transform and apply signal structures, *i.e.* constraints, in that domain, and alternate the operator, *i.e.* Fourier with inverse Fourier and vice versa, in the other iteration. We can interpret the Fourier and inverse Fourier transforms respectively as forward and backward operators. With some modifications we can instead use other forward/backward operator pairs, to impose the signal constraints in a custom sensing setting. We therefore use SAR forward and backward operators, *i.e.* $\mathcal{A}$ and $\mathcal{A}^H$.

We assume that the SAR imaging system provides us some erroneous phase history $\tilde{\mathbf{R}}_0$ as follows:

$$\tilde{\mathbf{R}}_0 = \mathbf{\Gamma}_0 \odot \mathcal{A}\mathbf{X}_0.$$

where we do not know the phase error matrix $\mathbf{\Gamma}_0$ and would like to retrieve $\mathbf{X}_0$ from such measurements. We therefore would like to find a pair $(\mathbf{\Gamma}^*, \mathbf{X}^*)$ that minimises the following program,

$$\min_{(\mathbf{\Gamma},\mathbf{X})} \|\tilde{\mathbf{R}}_0 - \mathbf{\Gamma} \odot \mathcal{A}\mathbf{X}\|_F.$$

To simplify the problem and make it suitable for volumetric SAR experiments, we choose a reference flight pass and would like to calibrate another flight pass phase history with respect to this data, to be able to coherently use the whole phase history. While other scenarios can be interesting, they need some extra requirements, *e.g.* existence of an isotropic target in the scene. We have another simplification: we assume that the (unknown) induced delay is fixed across the selected aperture, *i.e.* $\forall j, \epsilon_j = \epsilon$. This is a reasonable assumption for the short apertures, while it may not be correct for the large apertures. A solution is to break the long aperture to some smaller apertures, when it is possible. This approach has been prefered in some settings, where there are anisotropic target(s).

We start the GS framework with $\mathbf{\Gamma} = \mathbf{1}_{N\times J}$, where $\mathbf{1}_{N\times J}$ is the matrix with unit value elements, *i.e.* no phase error and initialise $\mathbf{X}_{ini} = \mathcal{A}^H\tilde{\mathbf{R}}_0$. The signal structure in the phase history domain can be applied by finding the best delay shift ϵ and using the following optimisation program,

$$\epsilon^* = \underset{\epsilon}{\operatorname{argmin}} \|\tilde{\mathbf{R}}_0 - \mathbf{\Gamma}_\epsilon \odot \mathcal{A}\mathbf{X}^{[k]}\|_F, \tag{2}$$

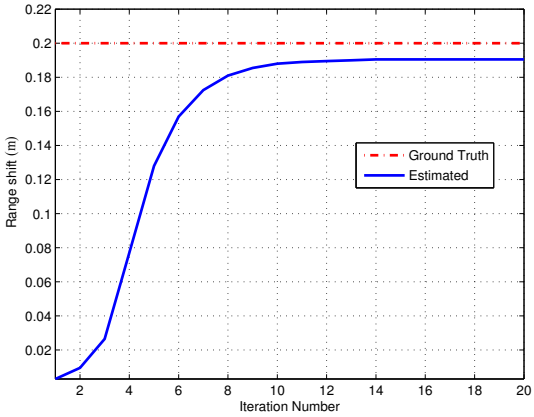

Fig. 4. The range error correction factor for synthetic experiment: estimated range (solid blue) and ground truth (dash-dot red).

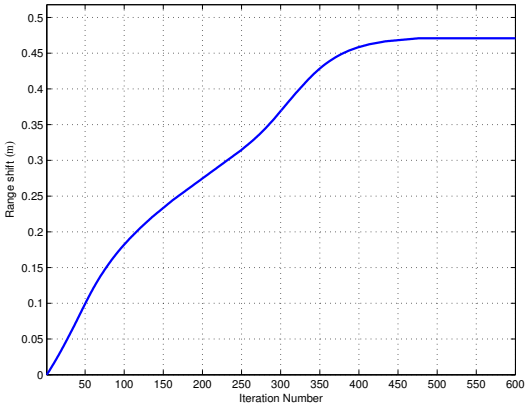

Fig. 5. The range error correction factor for QT corner reflector target.

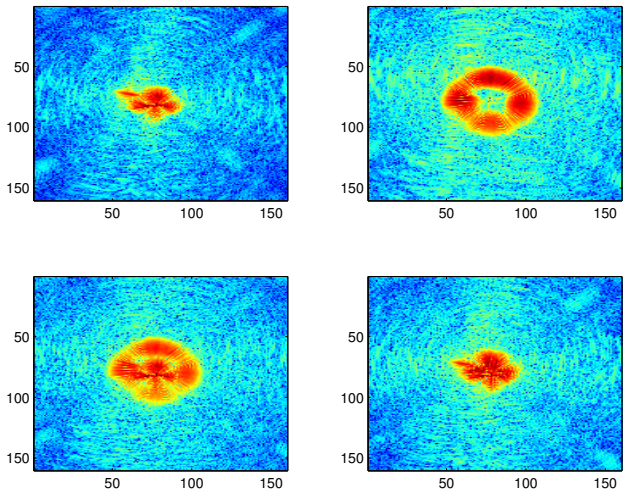

Fig. 6. Reconstructed SAR images of a Quad-Trihedral reference target with the back-projection algorithm using the phase history of: a) path number 1 (reference) top-left, b) path number 2 (with the range estimation error) top-right, c) coherent joint paths before correction, bottom-left, and d) after correction, bottom-right.

where $\mathbf{\Gamma}_\epsilon$ is the phase error matrix when $\boldsymbol{\epsilon} = \epsilon \mathbf{1}_J$ and $\mathbf{1}_J$ is a vector of length J with unit value elements. Solving this optimisation program looks difficult, but can be done by exhaustive or line search. As it is a one-dimensional program, it is a computationally tractable task. To induce the sparse (compressibility) structure of the reflectivity map $\mathbf{X}$, we simply soft-threshold [15] the back-projected ϵ^*-delayed phase history $\mathbf{X}^{[k+\frac{1}{2}]} = \mathcal{A}^H(\bar{\mathbf{\Gamma}}_{\epsilon^*} \odot \tilde{\mathbf{R}}_0)$, where bar sign indicate the complex conjugate, as follows:

$$\mathbf{X}_{p,q}^{[k+1]} = \max\left(|\mathbf{X}_{p,q}^{[k+\frac{1}{2}]}| - \frac{\lambda}{2}, 0\right).\mathrm{sign}(\mathbf{X}_{p,q}^{[k+\frac{1}{2}]}), \qquad (3)$$

where λ is the threshold parameter and sign operator is the projection onto the unit circle in the complex plane. λ controls the sparsity of the reflectivity map and its larger value makes more small values to become zero. This GS type algorithm continues by alternating between reflectivity map and phase-history and using (2) and (3) as induced structures until the new ϵ^* is roughly the same as its value in the previous iteration.

C. Simulation Results

The range estimation error has been observed in most raw data records, see for example [7], [10]. However, we initially set up some controlled synthetic simulations to show the potentials of the proposed range error correction algorithm in comparison with the ground truth information. We chose the general settings of the SAR multipass trial in [10] with a 4° aperture and a reflectivity map with four bright targets, to generate the phase history. The location of bright targets was selected at random, and we added some speckle noise to the reflectivity map to make it more realistic. We used the information about the pass numbers one and two, while phase history generated in the pass number one, did not have any range error and we induced a 20 cm range error to the pulses recorded in pass number two.

Figure 1 shows the back-projection image without any range error correction. A closer look at the image shows that the range error is in an order such that each bright target can be seen in two near, but connected, locations. We applied our algorithm and iterated 20 times. The final back-projected image with phase correction is shown in Figure 3. It is clear that this image is much sharper and focussed in a comparison with Figure 1. To demonstrate the algorithm capabilities in this experiment, we have plotted the estimated range error, in each iteration, in Figure 4. While we have started from an assumption that there is no range error, the algorithm managed to finally recover a parameter of 19 cm, which is close to the ground truth. The ground truth is shown with the red dash-dotted plot.

In the next experiment, we used the digitally chipped phase history of a Quad-Trihedral corner reflector [7]. The data set includes the data collected over 31 different circular orbits. We chose phase history data of two neighbour orbits, *i.e.* numbered 117 and 118, which are here respectively called the unfocussed (with some range estimation errors) and referenced. We chose such a setting as the path 118 has visually a minimum range estimation error, see top-left panel of Figure 6, compared to an error free QT back-projected image. The image generated using a phase history of an unfocused orbit is shown in the top-right panel of this figure, which clearly has some range estimation error, *i.e.* delay in dechirping. Coherent combination of the two phase history and imaging, do not increase the coherent gain, see the bottom-left panel of Figure 6. The combined phase history can be fed to the proposed algorithm to compensate the range estimation error of the unfocused part. The estimated range error in each iteration of the algorithm has been shown in Figure 5. The algorithm terminated after 600 iterations and an image reconstructed with the modified phase history, which has been shown in the bottom-right panel of Figure 6. Based on our observation, the number of

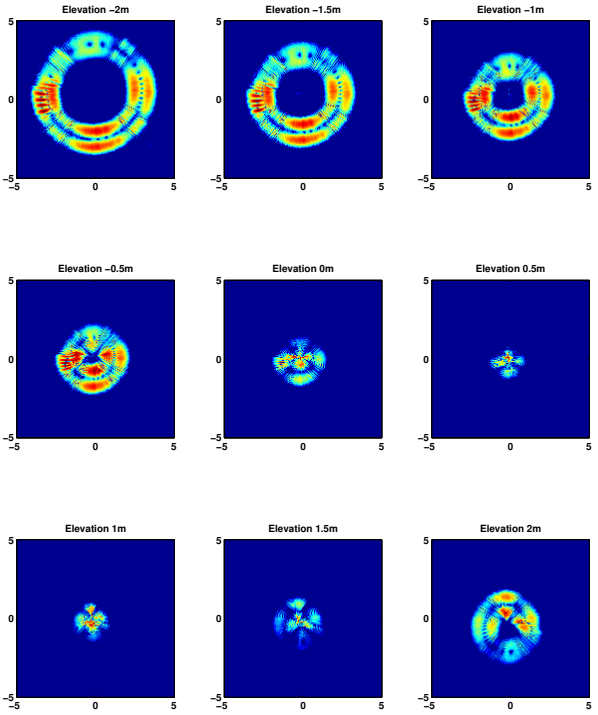

Fig. 7. Images formed using original phase history.

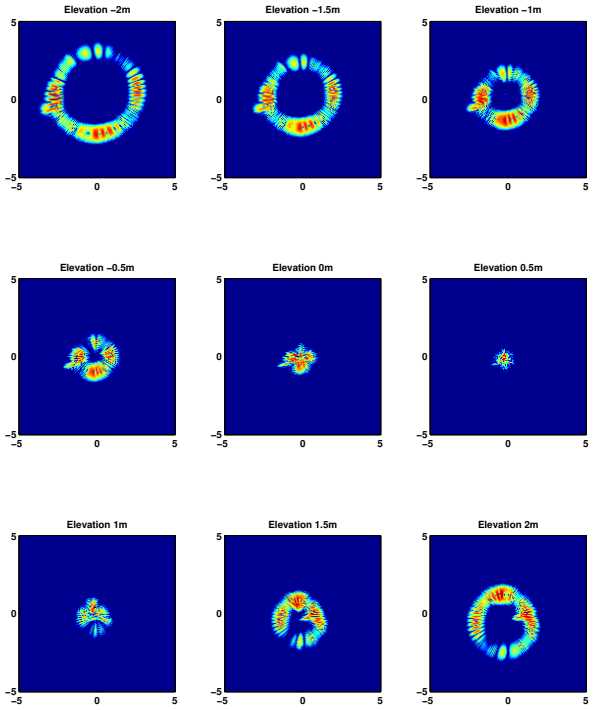

Fig. 8. Images formed using corrected phase history.

iterations before convergence is related to the thresholding parameter. It is clear from this figure that the proposed algorithm have managed to recover a suitable range error and focused the unfocussed phase history.

The modified phase history can be fed to a 3D-backprojection algorithm. In this setting, we have limited elevation resolution [16], as we have only used two orbits. The range estimation error causes a point target to be unfocussed on different elevations. This behaviour will roughly be observed in the QT corner reflectors. The formed images using the original phase history, which has range estimation errors, are shown in Figure 7. When the phase history is corrected, using the proposed method, the images will be more focussed, see Figure 8. It can be seen that the out-of-focus representation of the second pass data has been compensated.

D. Discussion

The problem of range estimation correction in a multipass SAR imaging was investigated here. The range error was modelled as a structured phase recovery problem. A new phase recovery algorithm was used to iteratively correct the error and focus the phase history for the coherent combination of pulses from different orbits. Further investigation of multi-orbit, *i.e.* more than two, an approach to select the thresholding parameter and volumetric reconstruction of the corrected phase history have been left for future work.

REFERENCES

[1] C. V. Jakowatz and D. E. Wahl, "Eigenvector method for maximum-likelihood estimation of phase errors in synthetic-aperture-radar imagery," *JOSA A*, vol. 10, no. 12, pp. 2539–2546, 1993.

[2] C. Mancill and J. Swiger, "A mapdrift autofocus technique for correcting higher order SAR phase errors," in *27th Annual Tri-Service Radar Symposium Record*, 1981, pp. 391–400.

[3] G. W. Donohoe, "Subaperture autofocus for synthetic aperture radar," *Aerospace and Electronic Systems, IEEE Transactions on*, vol. 30, no. 2, pp. 617–621, 1994.

[4] N. O. Onhon and M. Cetin, "A sparsity-driven approach for joint SAR imaging and phase error correction," *Image Processing, IEEE Transactions on*, vol. 21, no. 4, pp. 2075–2088, 2012.

[5] S. I. Kelly, M. Yaghoobi, and M. Davies, "Sparsity-based autofocus for undersampled synthetic aperture radar," *Aerospace and Electronic Systems, IEEE Transactions on*, vol. 50, no. 2, pp. 972–986, 2014.

[6] C. V. Jakowatz, D. E. Wahl, P. H. Eichel, D. C. Ghiglia, and P. A. Thompson, *Spotlight-Mode Synthetic Aperture Radar: A Signal Processing Approach: A Signal Processing Approach*. Springer Science & Business Media, 2012.

[7] K. E. Dungan, J. N. Ash, J. W. Nehrbass, J. T. Parker, L. A. Gorham, and S. M. Scarborough, "Wide angle SAR data for target discrimination research," in *SPIE Defense, Security, and Sensing*. International Society for Optics and Photonics, 2012, pp. 83 940M–83 940M.

[8] N. Boss, E. Ertin, and R. Moses, "Autofocus for 3d imaging with multipass SAR," in *SPIE Defense, Security, and Sensing*. International Society for Optics and Photonics, 2010, pp. 769 909–769 909.

[9] F. Lee-Elkin, "Autofocus for 3d imaging," in *SPIE Defense and Security Symposium*. International Society for Optics and Photonics, 2008, pp. 69 700O–69 700O.

[10] C. H. Casteel Jr, L. A. Gorham, M. J. Minardi, S. M. Scarborough, K. D. Naidu, and U. K. Majumder, "A challenge problem for 2d/3d imaging of targets from a volumetric data set in an urban environment," in *Defense and Security Symposium*. International Society for Optics and Photonics, 2007, pp. 65 680D–65 680D.

[11] K. E. Dungan and J. W. Nehrbass, "SAR focusing using multiple trihedrals," in *SPIE Defense, Security, and Sensing*. International Society for Optics and Photonics, 2013, pp. 874 606–874 606.

[12] T. J. Kragh, "Minimum-entropy autofocus for three-dimensional SAR imaging," in *SPIE Defense, Security, and Sensing*. International Society for Optics and Photonics, 2009, pp. 73 370B–73 370B.

[13] J. R. Fienup, "Phase retrieval algorithms: a comparison," *Applied optics*, vol. 21, no. 15, pp. 2758–2769, 1982.

[14] E. J. Candes, T. Strohmer, and V. Voroninski, "Phaselift: Exact and stable signal recovery from magnitude measurements via convex programming," *Communications on Pure and Applied Mathematics*, vol. 66, no. 8, pp. 1241–1274, 2013.

[15] D. Donoho and J. Johnstone, "Ideal spatial adaptation by wavelet shrinkage," *Biometrika*, vol. 81, no. 3, pp. 425–455, 1994.

[16] L. J. Moore and L. C. Potter, "Three-dimensional resolution for circular synthetic aperture radar," in *Defense and Security Symposium*. International Society for Optics and Photonics, 2007, pp. 656 804–656 804.